Struct Chem
DOI 10.1007/s11224-016-0809-7

ORIGINAL RESEARCH

Analysis of P–O–C, P–S–C and P–O–P angles: a database survey completed with four new X-ray crystal structures

Fahimeh Sabbaghi[1] · **Mehrdad Pourayoubi**[2] · **Michal Dušek**[3] · **Václav Eigner**[3] · **Sahar Bayat**[4] · **Krishnan Damodaran**[5] · **Marek Nečas**[6,7] · **Monika Kučeráková**[3]

Received: 31 March 2016 / Accepted: 18 July 2016

Abstract Four new crystal structures, $P(O)(OC_6H_5)_2(NHNHC_6H_5)$ (I), $P(S)(OCH_3)_2(NHCH(CH_3)_2)$ (II), $P(S)(OCH_3)_2$(NH-*cyclo*-C_5H_9) (III) and $[2\text{–}Cl\text{–}C_6H_4CH_2NH_3]_2[(CH_3S)P(O)(O)\text{–}O\text{–}P(O)(O)(SCH_3)]$ (IV) were studied. The P–O–C angles were analyzed, considering phosphoryl compound (I) and thiophosphoryl compounds (II) and (III) and their analogous structures deposited in the Cambridge Structural Database (CSD), including 282 $P(O)(O)_2(N)$ structures (706 P–O–C angles) and 186 $P(S)(O)_2(N)$ structures (518 P–O–C angles) with at least one P–O–C angle. The maximum populations of P–O–C angles are within 120°–122° in both $P(O)(O)_2(N)$ and $P(S)(O)_2(N)$ families of structures, confirming the hybridization state close to sp^2 for the oxygen atom of P–O–C. A survey on the CSD resulted in 11 $P(O)(O)_2(S\text{–}C)$ structures (11 P–S–C angles), and the structure (IV) belonging to this family of compounds is the first diffraction study of a salt with a (S)P(O)(O)–O–P(O)(O)(S) skeleton in the anion component. For the P–S–C angles, the maximum population was found in the range of 100°–104° showing the angles within those related to unhybridized pure *p* orbitals (p^3) and hybridized sp^3 for the sulfur atom of P–S–C. The analysis of 187 P(O)–O–P(O) structures (with no restriction on the other two atoms attached to phosphorus) including 538 P–O–P angles yielded the maximum population of P–O–P angles within 132°–134°, showing the more pronounced "*s*" character of the orbital (with respect to the sp^2 and toward *sp*) for the oxygen atom at the P–O–P moiety.

Keywords Cambridge Structural Database (CSD) · Crystal structure · Analysis of bond angle · Hybridization

Introduction

Organophosphorus compounds, especially of the pentavalent type, are extremely versatile and have prevalent environmental and industrial applications in agriculture and medicine [1]. They comprise two main groups, namely phosphoryl-based and thiophosphoryl-based compounds, with typical examples of phosphoramides and thiophosphoramides families containing the $P(O)[NR^1R^2]$ and $P(S)[NR^1R^2]$ moieties, respectively (R^1 and R^2 = H or a hydrocarbon) [2–7].

In various published papers, different structural features of phosphoramides [3–5], thiophosphoramides [6, 7] and complexes of phosphoryl donor ligands [8–10] were studied through diffraction experiments of their derivatives and investigation of analogous structures deposited in the Cambridge Structural Database (CSD [11]). Such studies help to gather the knowledge about these categories of

---

✉ Fahimeh Sabbaghi
fahimeh_sabbaghi@yahoo.com

[1] Department of Chemistry, Zanjan Branch, Islamic Azad University, Zanjan, Iran

[2] Department of Chemistry, Faculty of Sciences, Ferdowsi University of Mashhad, Mashhad, Iran

[3] Institute of Physics AS CR, v.v.i., Na Slovance 2, 182 21 Prague 8, Czech Republic

[4] Department of Chemistry, Payame Noor University, Zanjan, Iran

[5] Department of Chemistry, University of Pittsburgh, Pittsburgh, PA 15260, USA

[6] Department of Chemistry, Masaryk University, Kotlarska 2, 61137 Brno, Czech Republic

[7] CEITEC - Central European Institute of Technology, Masaryk University, Kamenice 5, 62500 Brno, Czech Republic

compounds, such as electronic properties of atoms and bonds [12–14], hybridization states of atoms in different parts of molecules [7, 14, 15], preferable conformations [7, 14], competition of different H-donor sites or H-acceptor sites in hydrogen bonding interactions [4, 12], and designing compounds with a desirable chemical structure [4]. The ultimate aim is prediction of crystal structures from molecular structures [4].

Among these studies, the geometries at the nitrogen atoms were analyzed in the structures with $(X)(Y)$N–P(=O) [14, 15] and $(X)(Y)$N–P(=S) [7] moieties (X, Y are any atoms from CSD, typically H, C and N). For these structures, the sums of valence angles ($\sum$) around nitrogen atoms (P–N–X + X–N–Y + Y–N–P) showed a tendency toward the sp^2 hybridization state, with most of the $\sum$ values near to the ideal sp^2 value of 360°. For a few structures with a distortion from a planar environment at the nitrogen atom, the proposed direction of lone electron pair (LEP) located on the nitrogen atom with respect to the P=O [14] or P=S [7] groups were discussed.

The N atom in a planar environment does not act as a hydrogen bond acceptor in crystal structure and shows low Lewis base character; however, the few examples of the N atom in a pyramidal environment do not show tendency as well. In fact, there are only a few structures with the N atom as an H-bond acceptor [16]. Moreover, a survey of the metal complexes on the CSD shows that the nitrogen atoms of the (X)(N)(Y)P=O and (X)(N)(Y)P=S moieties (X, Y are any atoms from CSD) have a very low tendency to bind the metal cations, too; so that, for example, in metal complex structures including a $P(S)(N)_3$-based ligand, it was only found a weak Sn···N interaction which was considered as a contact (not bond) in the corresponding paper [17].

Here, we focus on the geometries of the oxygen (esteratic and anhydride) and sulfur (thioesteratic) atoms bonded to phosphorus, considering four new crystal structures $P(O)(OC_6H_5)_2(NHNHC_6H_5)$ (I), $P(S)(OCH_3)_2(NHCH(CH_3)_2)$ (II), $P(S)(OCH_3)_2$(NH-*cyclo*-C_5H_9) (III) and [2–Cl–$C_6H_4CH_2NH_3]_2[(CH_3S)P(O)(O)$–O–$P(O)(O)(SCH_3)]$ (IV) and analogous structures from CSD with skeletons similar to (I), (II), (III) and (IV), i.e., with $P(O)(O)_2(N)$, $P(S)(O)_2(N)$, $P(O)(O)_2(S)$ and P(O)–O–P(O) skeletons. The structures from database are included in our investigation if they contain at least one P–O–C angle for the two first skeletons and one P–S–C angle for the third skeleton. There is no structure with a (S)P(O)(O)–O–P(O)(O)(S) skeleton [similar skeleton of compound (IV)] in the CSD, so the analysis of P–O–P angles was considered in all of the families of phosphorous compounds with a P(O)–O–P(O) skeleton with any restriction on the two other atoms bonded to each phosphorus atom in the skeleton. The structures (I) to (IV), selected for diffraction experiments, are suitable choices as the O and S atoms are not placed in a rigid environment allowing to have the geometries almost as were accessed by the nature of bonds and hybridization states of atoms.

The P–O–C, P–S–C and P–O–P bond angles are considered in these structures, and the histograms of distributions of angles are presented. Moreover, some compounds from CSD with interesting structural features are discussed in this paper and the chemical structures with the CSD refcodes are gathered in Table 1. This study can be used as a background for a discussion on the preferable hybridization states of O and S atoms attached to phosphorus. The Lewis base properties of such oxygen and sulfur atoms are also investigated here through a CSD analysis, in continuing the previous works done for the N atom attached to phosphorus [4].

Experimental

Materials and measurements

The chemicals $(C_6H_5O)_2P(O)Cl$, CH_3CN, $C_6H_5NHNH_2$, $CHCl_3$, CH_3OH, $(CH_3)_2CHNH_2$, $(CH_3O)_2P(S)Cl$, n-C_7H_{16}, *cyclo*-$C_5H_9NH_2$, 2-Cl-$C_6H_4CH_2NH_2$ and $CH_3C(O)CH_3$ were commercially available. Acetonitrile was dried with P_2O_5 and distilled prior to use. Previous articles mentioned the syntheses of (I) [18] and (III) [19] with together the ^{13}C NMR spectrum of (I) (DMSO-d_6) [20] and the ^{1}H and ^{31}P NMR of (III) ($CDCl_3$) [19]. Substance (II) exists in a patent [21] as well as in an article focusing on infrared spectroscopy of some P=S containing substances such as (II) [22], with no sign of any synthesis procedure in either of them. Other NMR experiments were not found in literature. The procedures reported here for compounds (I) and (III) are similar to the literature methods with a few modifications. Moreover, we further study these compounds with single crystal X-ray diffraction. The syntheses for the preparations of all four compounds began with the reagents being combined at ice-bath temperature, and the mixture then allowed coming to room temperature for the rest of the procedure. IR spectra were recorded on a Buck 500 scientific spectrometer using a KBr disk. ^{1}H, ^{13}C and ^{31}P NMR spectra were recorded on a FT-NMR Bruker Avance 300 spectrometer for compound (I) and on a Bruker Avance III 600 MHz NMR spectrometer for (II) and (III). ^{1}H and ^{13}C NMR spectra were referenced using the solvent DMSO-d_6 resonances (2.50 and 39.52 ppm for ^{1}H and ^{13}C, respectively), and ^{31}P NMR spectra were calibrated using "absolute referencing" from the ^{1}H spectrum. For (I), (II) and (IV), data collection was obtained at 120 K on a single crystal diffractometer Gemini using mirrors-collimated Cu-$K\alpha$ radiation ($\lambda = 1.5418$ Å). For (III), data were collected at 120 K on a Rigaku MicroMax-007 HF rotating anode CCD diffractometer using Mo-$K\alpha$ radiation ($\lambda = 0.71073$ Å). The structures were solved by the charge flipping algorithm of

Table 1 Chemical structures of refcodes (arranged alphabetically) discussed in the text

ATEXAY01	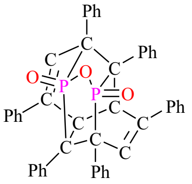	HAXQOO	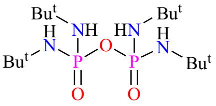
BEVGAK	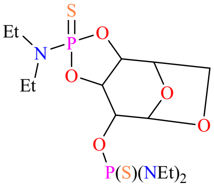	HAXRAZ	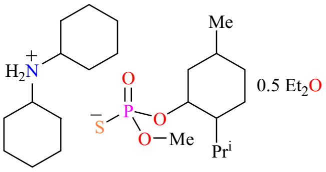
BOKSUP	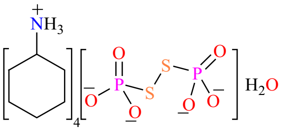	IJUMAB	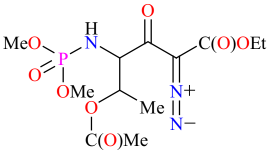
DANHIJ	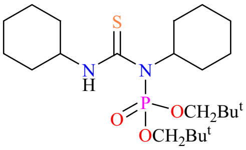	KIVFAW	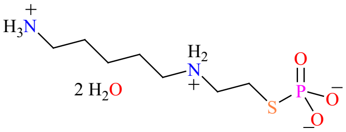
DANMAG	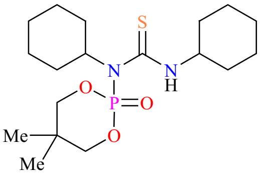	MAXDOG	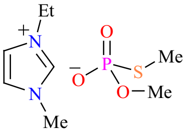
DUPCOH	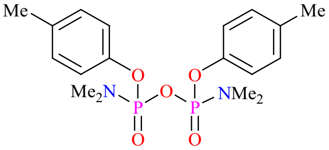	PALWUU	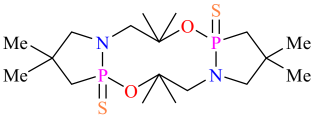
EPGUAN10	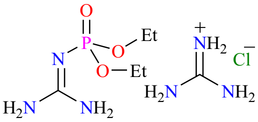	SOYRAZ	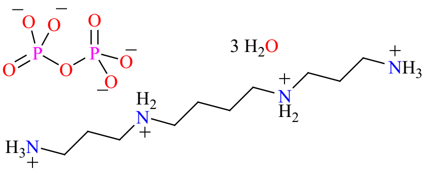
GEYMUS	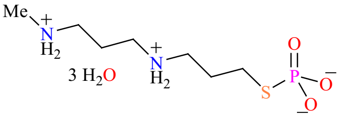		

Table 2 Crystallographic data and structure refinement details for (I) and (II)

	(I)	(II)
Empirical formula	$C_{18}H_{17}N_2O_3P$	$C_5H_{14}NO_2PS$
Formula weight	340.3	183.2
Temperature (K)	120.00 (10)	120.00 (10)
Wavelength (Å)	1.54184	1.54184
Crystal system	Monoclinic	Triclinic
Space group	$P2_1/n$	P–1
Unit cell dimension		
a (Å)	13.5418 (10)	6.5734 (5)
b (Å)	5.9725 (3)	8.8944 (5)
c (Å)	21.2750 (13)	9.3128 (8)
α (°)	90	118.121 (8)
β (°)	105.791 (6)	101.560 (7)
γ (°)	90	91.243 (6)
V (Å^3)	1655.75 (19)	466.20 (7)
Z	4	2
Calculated density (g cm^{-3})	1.3648	1.3051
Index ranges	$-15 \leq h \leq 14$	$-6 \leq h \leq 7$
	$-6 \leq k \leq 5$	$-8 \leq k \leq 10$
	$-23 \leq l \leq 25$	$-10 \leq l \leq 9$
F (000)	712	196
θ range for data collection (°)	3.49–67.06	5.55–66.83
Max. and min. transmission	0.891 and 0.624	1 and 0.827
Goodness of fit on F^2	1.95	1.30
Reflections measured/independent/R_{int}	5564/2862/0.0475	2739/1599/0.0316
Final R factors [number of independent observed reflections][a]	$R_1 = 0.0671$, $wR_2 = 0.1637$ [2259]	$R_1 = 0.0300$, $wR_2 = 0.0369$ [1395]
Absorption coefficient (mm^{-1})	1.631	4.328
Largest difference in peak and hole (e Å^{-3})	0.57 and −0.41	0.21 and −0.21

[a] The observability limit is $I > 3\sigma(I)$ for (I) and (II)

Superflip [23] and refined by Jana 2006 [24]. MCE software [25] was used for visualization of electron density maps. In case of structure (I), the disordered phenyl group was refined using rigid body refinement with occupancy constrained to full. The resulting occupancy ratio was 0.547 (3):0.453 (3). In case of non-centrosymmetric structure (IV), Flack parameter [26] was refined to final value 0.32 (2). Since the compound is not a single enantiomer, the unambiguous value is not an issue. Further details of X-ray analysis and data collection for structures (I) & (II) and (III) & (IV) are given in Tables 2 and 3, and selected bond lengths and angles are given in Tables 4 and 5.

Syntheses

$P(O)(OC_6H_5)_2(NHNHC_6H_5)$ (I)

Phenylhydrazine, $C_6H_5NHNH_2$, was added slowly to a stirred solution of $(C_6H_5O)_2P(O)Cl$ (2:1 mol ratio) in CH_3CN at ice-bath temperature. After 4 h, the solvent was removed and the solid residue was washed with distilled water. Single crystals were obtained from $CH_3CN/CHCl_3/CH_3OH$ (1:1:2 *v*/*v*/*v*) by slow evaporation at room temperature. IR (KBr, cm^{-1}): 3296, 3211, 3050, 2874, 1943, 1871, 1793, 1596, 1520, 1490, 1454, 1308, 1229, 1190, 1158, 1073, 1019, 969, 888, 851, 774, 756, 688. $^{31}P\{^1H\}$ NMR (121 MHz, DMSO-d_6): $\delta = -1.49$ (s). ^1H NMR (300 MHz, DMSO-d_6): $\delta = 6.69$ (t, $^3J_{H-H} = 7.2$ Hz, 1H), 6.80 (d, $^3J_{H-H} = 8.3$ Hz, 2H), 7.09 (t, $^3J_{H-H} = 8.1/7.5$ Hz, 2H), 7.21 (m, 6H), 7.39 (t, $^3J_{H-H} = 8.1/7.5$ Hz, 4H), 7.60 (d, $^3J_{H-P} = 3.9$ Hz, 1H, NH), 7.92 (d, $^2J_{H-P} = 41.2$ Hz, 1H, NH). ^{13}C NMR (75 MHz, DMSO-d_6): $\delta = 112.69$ (s, C^6 (*ortho*)), 118.70 (s, C^8 (*para*)), 120.35 (d, $^3J_{C-P} = 4.7$ Hz, C^2 (*ortho*)), 124.92 (s, C^4 (*para*)), 128.47 (s, C^7 (*meta*)), 129.76 (s, C^3 (*meta*)), 149.59 (d, $^3J_{C-P} = 4.8$ Hz, C^5 (*ipso*)), 150.57 (d, $^2J_{C-P} = 6.9$ Hz, C^1 (*ipso*)). The C^1 to C^4 and C^5 to C^8 correspond to the C_6H_5O and C_6H_5NHNH groups, respectively.

Table 3 Crystallographic data and structure refinement details for (III) and (IV)

	(III)	(IV)
Empirical formula	$C_7H_{16}NO_2PS$	$C_2H_6O_5P_2S_2$, $2(C_7H_9ClN)$
Formula weight	209.24	521.4
Temperature (K)	120 (2)	120.01 (10)
Wavelength (Å)	0.71073	1.54184
Crystal system	Triclinic	Monoclinic
Space group	*P*–1	$P2_1$
Unit cell dimension		
a (Å)	12.0681 (3)	8.5464 (3)
b (Å)	12.2552 (3)	11.9725 (4)
c (Å)	14.8655 (4)	11.7919 (5)
α (°)	72.414 (2)	90
β (°)	83.442 (2)	105.161 (3)
γ (°)	88.509 (2)	90
V ($Å^3$)	2082.01 (9)	1164.57 (8)
Z	8	2
Calculated density (g cm^{-3})	1.335	1.4868
Index ranges	$-15 \leq h \leq 15$	$-9 \leq h \leq 10$
	$-16 \leq k \leq 15$	$-14 \leq k \leq 13$
	$-20 \leq l \leq 19$	$-13 \leq l \leq 13$
F (000)	896	540
θ range for data collection (°)	1.7–29.7	3.88–67.06
Max. and min. transmission	1.00 and 0.88	0.599 and 0.272
Goodness of fit on F^2	1.30	1.74
Reflections measured/independent/R_{int}	24,922/10,008/0.0304	8259/4048/0.0569
Final *R* factors [number of independent observed reflections][a]	$R_1 = 0.0361$, $wR_2 = 0.0937$ [7331]	$R_1 = 0.0480$, $wR_2 = 0.1085$ [3843]
Absorption coefficient (mm^{-1})	0.429	5.724
Largest difference in peak and hole (e $Å^{-3}$)	0.33 and −0.31	0.51 and −0.31

[a] The observability limit is $I > 3\sigma(I)$ for (III) and (IV)

$P(S)(OCH_3)_2(NHCH(CH_3)_2)$ (II)

Iso-propylamine, $(CH_3)_2CHNH_2$, was added slowly to a stirred solution of $(CH_3O)_2P(S)Cl$ (2:1 mol ratio) in CH_3CN at ice-bath temperature. After 4 h, the solvent was removed and the solid formed was washed with distilled water. Single crystals were obtained from a solution of product in a mixture of $CHCl_3$/n-C_7H_{16} (4:1 *v*/*v*). IR (KBr, cm^{-1}): 3312, 2971, 2721, 2615, 2471, 1841, 1460, 1416, 1378, 1316, 1176, 1133, 1061, 902, 837, 781, 643. $^{31}P\{^1H\}$ NMR (243 MHz, DMSO-d_6): $\delta = 74.83$ (s). ^1H NMR (601 MHz, DMSO-d_6): $\delta = 1.06$ (dd, $J = 6.6$, 0.7 Hz, 6H), 3.29 (ddh, $J = 10.3$, 9.5, 6.5 Hz, 1H), 3.54 (d, $^3J_{H–P} = 13.6$ Hz, 6H), 5.45 (dd, $J = 15.1$, 9.5 Hz, 1H, NH). ^{13}C NMR (151 MHz, DMSO-d_6): $\delta = 24.68$ (d, $^3J_{C–P} = 5.7$ Hz, $CH(\underline{C}H_3)_2$), 43.82 (d, $^2J_{C–P} = 1.7$ Hz, CH), 52.62 (d, $^2J_{C–P} = 5.1$ Hz, $\underline{C}H_3O$).

$P(S)(OCH_3)_2(NH$-cyclo-$C_5H_9)$ (III)

Cyclopentylamine, *cyclo*-$C_5H_9NH_2$, was added slowly to a stirred solution of $(CH_3O)_2P(S)Cl$ (2:1 mol ratio) in CH_3CN at ice-bath temperature. After 4 h, the solvent was removed and the solid formed was washed with distilled water. Single crystals were obtained from a solution of product in a mixture of CH_3OH/CH_3CN (1:1 *v*/*v*) by slow evaporation at room temperature. IR (KBr, cm^{-1}): 3314, 2954, 2867, 1743, 1436, 1281, 1178, 1107, 1029, 936, 810, 645. $^{31}P\{^1H\}$ NMR (243 MHz, DMSO-d_6): $\delta = 75.16$ (s). ^1H NMR (601 MHz, DMSO-d_6): $\delta = 1.32$–1.40 (m, 2H), 1.40–1.47 (m, 2H), 1.56–1.66 (m, 2H), 1.71–1.81 (m, 2H), 3.39–3.46 (m, 1H), 3.54 (d, $^3J_{H–P} = 13.6$ Hz, 6H), 5.55 (dd, $J = 15.4$, 9.2 Hz, 1H, NH). ^{13}C NMR (151 MHz, DMSO-d_6): $\delta = 22.85$ (s, CH_2), 33.80 (d, $^3J_{C–P} = 5.7$ Hz, CH_2), 52.57 (d, $^2J_{C–P} = 4.9$ Hz, CH_3), 53.37 (d, $^2J_{C–P} = 2.3$ Hz, CH).

Table 4 Selected geometric parameters for (I) and (II)

Compound (I)			
P1–O1	1.471 (2)	O3–C1b	1.403 (4)
P1–O2	1.575 (2)	O3–C1c	1.410 (5)
P1–O3	1.573 (3)	N1–N2	1.406 (4)
P1–N1	1.615 (3)	N2–C1d	1.431 (4)
O2–C1a	1.406 (4)		
O1–P1–O2	114.38 (14)	O3–P1–N1	103.11 (15)
O1–P1–O3	116.30 (14)	P1–O2–C1a	119.75 (18)
O1–P1–N1	110.15 (13)	P1–O3–C1b	125.0 (3)
O2–P1–O3	100.44 (13)	P1–O3–C1c	128.4 (3)
O2–P1–N1	111.67 (14)	P1–N1–N2	120.1 (2)
N1–N2–C1d	116.3 (3)	O2–C1a–C2a	119.1 (3)
Compound (II)			
P1–S1	1.9390 (7)	O1–C4	1.451 (4)
P1–O1	1.5819 (16)	O2–C5	1.446 (3)
P1–O2	1.5853 (13)	N1–C1	1.484 (3)
P1–N1	1.614 (2)		
S1–P1–O1	114.90 (7)	O2–P1–N1	107.30 (10)
S1–P1–O2	115.07 (6)	P1–O1–C4	119.05 (13)
S1–P1–N1	112.87 (5)	P1–O2–C5	119.53 (11)
O1–P1–O2	99.12 (7)	P1–N1–C1	125.83 (13)
O1–P1–N1	106.34 (9)	N1–C1–C3	108.35 (15)

$[2\text{-Cl-}C_6H_4CH_2NH_3]_2[(CH_3S)P(O)(O)\text{–}O\text{–}P(O)(O)(SCH_3)]$ (IV)

A procedure similar to the one described for (II) and (III) was used; however, the hydrolysis happened in the synthesis process (due to a few moisture remained in CH_3CN) to yield the pyrophosphate (IV). 2-Chlorobenzylamine, $2\text{-Cl-}C_6H_4CH_2NH_2$, was added slowly to a stirred solution of $(CH_3O)_2P(S)Cl$ (2:1 mol ratio) in CH_3CN at ice-bath temperature. After 4 h, the solvent was removed and the solid formed was washed with distilled water. Single crystals, suitable for X-ray crystallography, were obtained from a solution of product in a $CHCl_3/CH_3C(O)CH_3/CH_3OH$ mixture (1:1:1 *v*/*v*/*v*) by slow evaporation at room temperature. The re-arrangement in the $(CH_3O)P(S)(O)$ fragment and transformation to $(CH_3S)P(O)(O)$ is surprising. As the product was fortuitously obtained, good NMR data were not recorded. IR (KBr, cm^{-1}): 2170–3147 (b), 2975, 2938, 2747, 2672, 2612, 1730, 1478, 1394, 1243, 1175, 1036, 896, 850, 806, 754, 694.

Table 5 Selected geometric parameters for (III) and (IV)

Compound (III)			
S1a–P1a	1.9346 (6)	S1c–P1c	1.9336 (6)
P1a–O2a	1.5848 (11)	P1c–O2c	1.5807 (11)
P1a–O1a	1.5880 (14)	P1c–O1c	1.5869 (14)
P1a–N1a	1.6152 (15)	P1c–N1c	1.6141 (15)
N1a–C1a	1.476 (2)	N1c–C1c	1.479 (2)
O1a–C6a	1.446 (2)	O1c–C6c	1.447 (2)
O2a–C7a	1.4499 (19)	O2c–C7c	1.454 (2)
S1b–P1b	1.9367 (6)	S1d–P1d	1.9341 (6)
P1b–O2b	1.5842 (14)	P1d–O2d	1.5841 (14)
P1b–O1b	1.5795 (11)	P1d–O1d	1.5807 (11)
P1b–N1b	1.6145 (15)	P1d–N1d	1.6142 (16)
N1b–C1b	1.469 (2)	N1d–C1d	1.471 (2)
O1b–C6b	1.454 (2)	O1d–C6d	1.450 (2)
O2b–C7b	1.446 (2)	O2d–C7d	1.441 (2)
O2a–P1a–O1a	98.85 (6)	O2c–P1c–O1c	99.21 (6)
O2a–P1a–N1a	104.48 (7)	O2c–P1c–N1c	104.75 (7)
O1a–P1a–N1a	108.09 (8)	O1c–P1c–N1c	107.31 (8)
O2a–P1a–S1a	115.37 (5)	O2c–P1c–S1c	115.25 (5)
O1a–P1a–S1a	114.80 (5)	O1c–P1c–S1c	114.35 (5)
N1a–P1a–S1a	113.77 (5)	N1c–P1c–S1c	114.45 (5)
C1a–N1a–P1a	125.21 (11)	C1c–N1c–P1c	123.52 (11)
C6a–O1a–P1a	119.51 (10)	C6c–O1c–P1c	118.71 (10)
C7a–O2a–P1a	119.29 (10)	C7c–O2c–P1c	119.61 (10)
O2b–P1b–O1b	99.33 (6)	O2d–P1d–O1d	99.15 (6)
O2b–P1b–N1b	106.41 (8)	O2d–P1d–N1d	106.73 (8)
O1b–P1b–N1b	105.97 (7)	O1d–P1d–N1d	105.86 (7)
O2b–P1b–S1b	115.24 (5)	O2d–P1d–S1d	114.72 (5)
O1b–P1b–S1b	115.27 (5)	O1d–P1d–S1d	115.43 (5)
N1b–P1b–S1b	113.25 (5)	N1d–P1d–S1d	113.56 (5)
C1b–N1b–P1b	124.98 (11)	C1d–N1d–P1d	124.73 (11)
C6b–O1b–P1b	119.27 (10)	C6d–O1d–P1d	119.48 (10)
C7b–O2b–P1b	119.01 (10)	C7d–O2d–P1d	119.39 (10)
Compound (IV)			
P1–S1	2.0732 (13)	P2–O4	1.473 (3)
P1–O1	1.489 (3)	P2–O5	1.487 (3)
P1–O2	1.482 (3)	N1a–C7a	1.497 (7)
P2–S2	2.0832 (14)	N1b–C7b	1.489 (7)
S1–P1–O1	110.88 (13)	S2–P2–O5	106.91 (14)
S1–P1–O2	106.59 (14)	O4–P2–O5	117.55 (16)
O1–P1–O2	119.51 (17)	N1a–C7a–C2a	112.7 (4)
S2–P2–O4	110.35 (13)	N1b–C7b–C2b	114.0 (4)

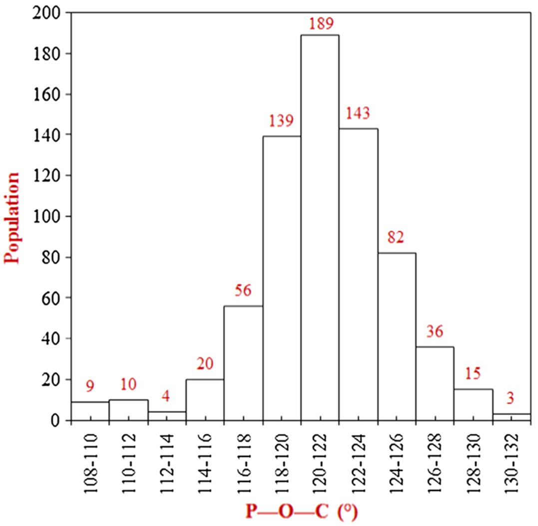

Fig. 1 Histogram of P–O–C angles in structures with a P(O)(O–C)$_{2-x}$(O)$_x$(N) fragment ($x = 0, 1$) deposited in the CSD

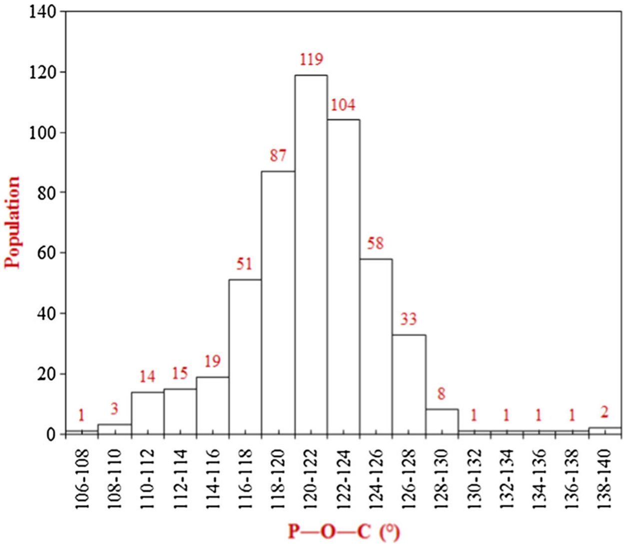

Fig. 2 Histogram of P–O–C angles in structures with a P(S)(O–C)$_{2-x}$(O)$_x$(N) fragment ($x = 0, 1$) deposited in the CSD

Results and discussion

CSD analysis

Analysis of P–O–C bond angles in compounds with a P(O)(O–C)$_{2-x}$(O)$_x$(N) fragment ($x = 0, 1$)

The P–O–C bond angles were analyzed for compounds with a similar skeleton to compound (I), i.e., P(O)(O)$_2$(N), and including at least one P–O–C angle. The CSD in version 5.37 (updated in February 2016) was applied, and the search filters were used to remove metal complexes, compounds without any P–O–C bond angle, duplicated structures based on the same diffraction data and the structures with disorder in the target angle. So, the set of 282 structures with P–O–C bond angles was finally considered in our study. The P–O–C bond angles vary in the range of 108°–132° with the maximum population within 120°–122° (189 hits of the total hits of 706, about 27 %), shown as histogram in Fig. 1. The maximum population of angles is near to the angle of sp^2 orbitals, similar to what was previously found for the P–N–C angles in P(O)(N)$_3$ [14] and P(S)(N)$_3$ [7] structures with the N atom in a three-coordinate (P)N(X)(Y) environment, X = C, Y is any atom from CSD.

Analysis of P–O–C bond angles in compounds with a P(S)(O–C)$_{2-x}$(O)$_x$(N) fragment ($x = 0, 1$)

The P–O–C bond angles were also analyzed for compounds with a similar skeleton to compounds (II) and (III), i.e., P(S)(O)$_2$(N)-based structures, and including at least one P–O–C angle. After applying criteria similar to what was noted in the previous section, the set of 186 structures was considered for analysis. The P–O–C bond angles vary in the range of 106°–140° with the maximum population in the similar region of P(O)(O)$_2$(N)-based structures within 120°–122° (119 hits of the total hits of 518, about 23 %). The histogram is shown in Fig. 2. The data in the P(S)(O)$_2$(N) structures are spread in a wider range with respect to the data for the P(O)(O)$_2$(N) structures, due to diverse types of structures within this family of compounds. For example, the minimum P–O–C angle is related to the compound with refcode BEVGAK [27] which includes the noted angle in a five-member heterocyclic ring, and the maximum value is related to the structure with refcode PALWUU [28] with a ten-member heterocyclic ring. The chemical structures of refcodes discussed are given in Table 1.

Analysis of P–S–C bond angles in compounds with a P(O)(O)$_2$(S–C) fragment

For a comparison with P–O–C, the P–S–C bond angles were analyzed for the compounds with the same skeleton to the compound (IV), i.e., P(O)(O)$_2$(S). The CSD yielded only 11 relevant structures (11 P–S–C angles), including a P(O)(O)$_2$(S–C) fragment, with the P–S–C bond angles within 97.4°–104.8°. As a few data exist in the CSD for this skeleton, the histogram was not considered. For these data, 8 hits are within 100°–104° which are significantly (about 20°) less than the maximum population of bond angles found for the P–O–C angles in both two previously mentioned families. The P–S–P and P–S–S angles were also found in the P(O)(O)$_2$(S) structures from the CSD (5 hits in 4 structures) ranging from 102.2° to 108.8°. The differences between P–S–P angles (the average value of 103.6°

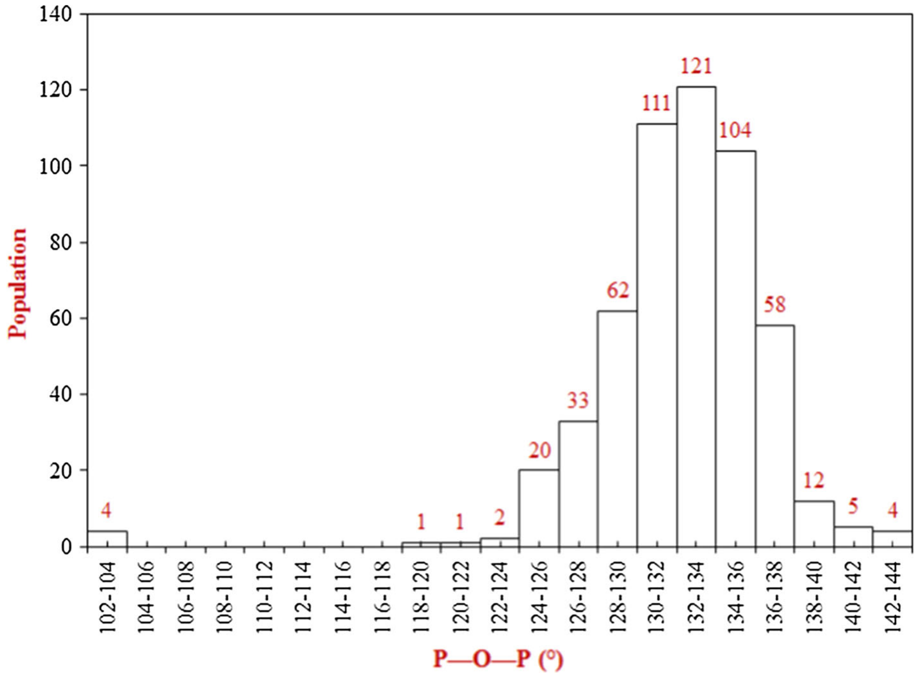

Fig. 3 Histogram of P–O–P angles in structures with a P(O)–O–P(O) skeleton deposited in the CSD

for 3 hits) with those of P–O–P angles (around 130°, discussed in the next section) are also significant.

Analysis of P–O–P bond angles

The P–O–P bond angles were analyzed for the compounds with a P(O)–O–P(O) skeleton with any restriction on the other two atoms attached to phosphorus. A dataset of 187 relevant structures including 538 P–O–P bond angles was used for this discussion. The P–O–P bond angles vary in the range of 102°–144° with the maximum population at 132°–134° (121 hits, about 22 %), shown as histogram in Fig. 3. The minimum value is related to a cyclic compound (refcode ATEXAY01 [29]), and the maximum value is related to a cation–anion structure with refcode SOYRAZ [30]. It seems that the involvement of all of the terminal oxygen atoms of the $[(O)_3P–O–P(O)_3]^{-4}$ anion is responsible to such a high P–O–P angle in SOYRAZ. The data of P–O–P angles are more concentrated within 124°–140° (about 97 %), and also there is not any data within 104°–118°. The bond angles at the maximum populations are in accordance with the hybridization with more participation of "*s*" orbital compared to the sp^2 for the oxygen atom at the P–O–P moiety.

Hydrogen bonding interactions involving in the oxygen and sulfur atoms of the noted structures

A CSD analysis on compounds with a P(O)(O)$_2$(N) skeleton and with at least one NH or OH unit and also at least with one P–O–C shows that the oxygen atom of P–O–C (O_{CP}) does not act as a hydrogen bond acceptor showing its low Lewis base character. Only four exceptions were found out of 175 structures. In one of these structures (DANHIJ [31]), the NH unit involves in N–H(···O=P)(···O_{CP}) hydrogen bond. In the structure with CSD refcode DANMAG [32], the spatial distances between the N atom with two oxygen atoms (below 3 Å) also propose the N–H(···O=P)(···O_{CP}) hydrogen bond; however, it does not have hydrogen atoms positions determined, and the judgment is along with caveat. In one other structure (EPGUAN10 [33]), five NH_2 units are present and all of

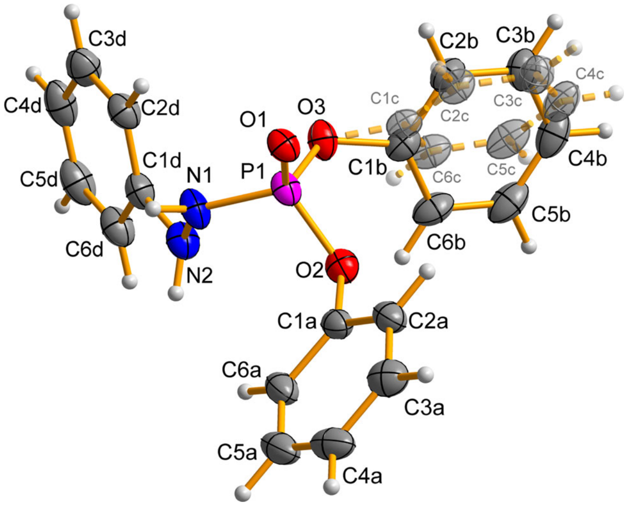

Fig. 4 Displacement ellipsoid plot (50 % probability) is shown for (I) with atom numbering scheme. H atoms are drawn as spheres of arbitrary radii. *Dashed lines* indicate disordered C_6H_5 ring

the sites possible for hydrogen bond acceptor capability (N, Cl and the oxygen atoms of P=O and P–O–C) take part in hydrogen bonding interaction. In the remaining structure (IJUMAB [34]), the P=O group takes part in the (C–H···)(C–H···)O hydrogen bonding and the O_{CP} atom takes part in a week N–H···O hydrogen bond interaction. This finding is due to the better hydrogen bond acceptor capability of the oxygen atom of P=O group versus the oxygen atom of P–O–C. This is similar to the low Lewis base characteristic of the nitrogen atom of $P(O)(N)_3$, which was studied through a CSD analysis [3].

A similar analysis for compounds with a $P(S)(O)_2(N)$ skeleton and including at least one NH or OH unit and at least one P–O–C was performed for a comparison between the hydrogen bond acceptor capability of the sulfur atom of P=S group and the oxygen atom of P–O–C fragment. From 120 structures, 49 structures include the N–H···S=P hydrogen bond (and one structure includes O–H···S=P hydrogen bond), while 17 structures include N–H···O_{CP} hydrogen bond. This analysis shows, however, the sulfur atom makes a weak hydrogen bond, but the hydrogen bond acceptor capability of sulfur atom of P=S group is larger than one for the oxygen atom of P–O–C. The differences in the hydrogen bond acceptor capabilities of P=S and O_{CP} are less than the differences found in comparing P=O group and O_{CP} atom. Among the structures noted, 2 ones show both N–H···S=P and N–H···O_{CP} hydrogen bonds. In the remaining 55 structures, there are other acceptor groups which take part in hydrogen bonding interaction or the compound does not show the classical hydrogen bond. These observations are important in crystal engineering concepts for structures with P(O)(O–C)(NH) and P(S)(O–C)(NH) moieties: While in the former, the P=O group dominates the hydrogen bond pattern as a prominent hydrogen bond acceptor, there is a competition between P=S and O_{CP} in the latter moiety with only slightly better capability for accepting H atom by P=S group.

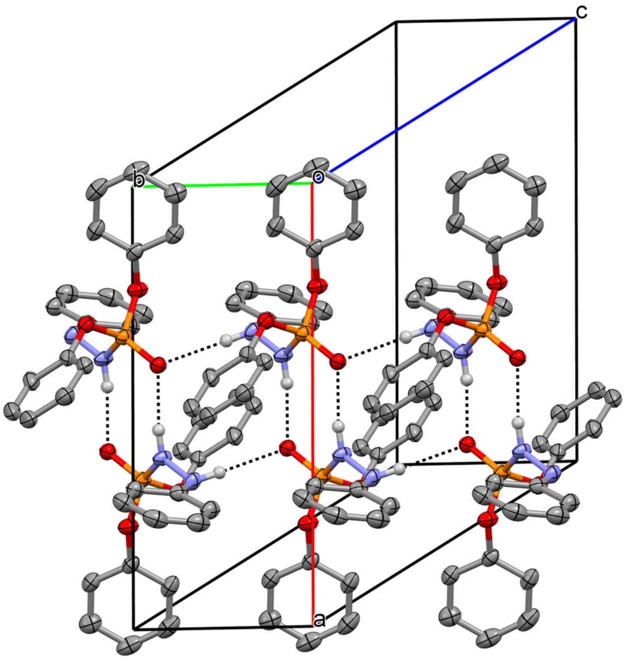

Fig. 5 Crystal packing for structure (I), the N–H···O=P hydrogen bonds are shown as *dashed lines*. The weakly occupied atoms and hydrogen atoms not involved in hydrogen bonding were omitted for the sake of clarity

Table 6 Hydrogen bond geometry (Å, °) for compound (I)

D–H···*A*	*D*–H	H···*A*	*D*···*A*	*D*–H···*A*
N1–H1n1···O1^a	0.881 (15)	2.035 (15)	2.911 (4)	173 (4)
N2–H1n2···O1^b	0.88 (3)	2.22 (3)	3.095 (4)	172 (3)
C6d–H1c6d···O3^b	0.96	2.41	3.354 (5)	168.55

Symmetry codes: ^{a} $-x+1, -y, -z$; ^{b} $x, y-1, z$

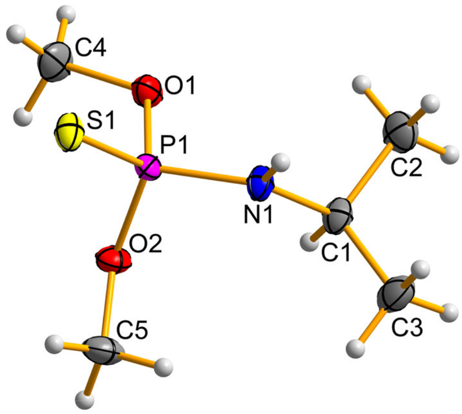

Fig. 6 Displacement ellipsoid plot (50 % probability) is shown for (II) with atom numbering scheme. H atoms are drawn as spheres of arbitrary radii

X-ray crystallography experiments for new structures

Structure (I) was studied as an example including the P atom within a distorted tetrahedral $P(O)(O)_2(N)$ environment (Fig. 4). The P=O and P–N bond lengths [of 1.471 (2) and 1.615 (3) Å, respectively] are within the standard ranges for analogous compounds [12]. The bond angles at the P atom vary in the range 100.44 (13)° [O2–P1–O3] to 116.30 (14)° [O1–P1–O3]. Of the two N atoms in the C_6H_5NHNH group, atom N2 has more pronounced sp^3-hybridization relative to atom N1, which is almost perfectly planar environment (the bond angle sums are 349 (2)° and

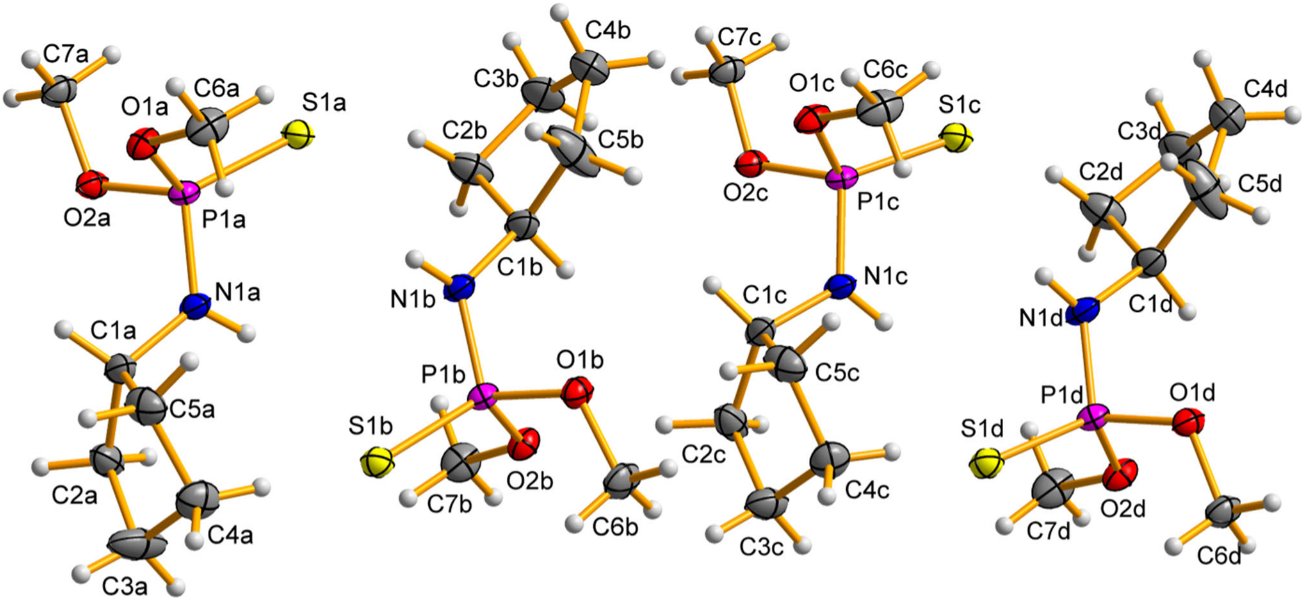

Fig. 7 Displacement ellipsoid plot (50 % probability) is shown for structure (III) with atom numbering scheme. H atoms are drawn as spheres of arbitrary radii

359 (3)°, respectively). The P1–O2–C1a bond angle is 119.75 (18)°, and the other OC_6H_5 group indicates disorder over two sites. The resulting occupancy ratio of disordered phenyl positions was refined as 0.547 (3):0.453 (3). In the crystal structure, molecules are linked via (N–H···)(N–H···)O=P hydrogen bonds into a one-dimensional arrangement parallel to the *b* axis (Fig. 5; Table 6). This arrangement includes alternating $R_2^2(8)$ and $R_4^2(10)$ hydrogen-bonded ring motifs (for graph-set notation, see Ref. [35]).

For a comparison with compound (I), compounds (II) and (III) including $P(S)(O)_2(N)$ skeleton were synthesized. The asymmetric unit of (II) is composed of one complete molecule (Fig. 6), and for (III) it contains four symmetry independent molecules (Fig. 7). The P=S bond lengths [of 1.9390 (7) Å for (II) and 1.9346 (6), 1.9367 (6), 1.9336 (6) and 1.9341 (6) Å for (III)] are within the expected values for compounds with a $P(S)(O)_2(N)$ skeleton [6]. The P–N bond lengths [of 1.614 (2) Å for (II) and 1.6152 (15), 1.6145 (15), 1.6141 (15) and 1.6142 (16) Å, for (III)] are within the expected range for $P(S)(O)_2(N)$-based structures and are shorter than the maximum population of P–N bonds found for $P(S)(N)_3$-based structures [6].

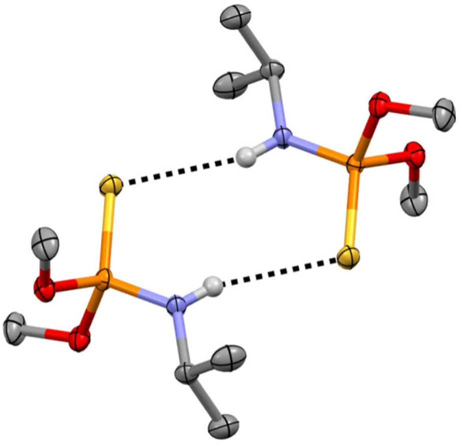

Fig. 8 A view of centrosymmetric dimer in structure (II) built from a pair of N–H···S=P hydrogen bonds

Table 7 Hydrogen bond geometry (Å, °) for compound (II)

D–H···*A*	*D*–H	H···*A*	*D*···*A*	*D*–H···*A*
N1–H1N1···S1[a]	0.82 (2)	2.68 (3)	3.4770 (19)	163 (3)

Symmetry code: [a] $-x + 2, -y + 1, -z + 1$

In structure (II), the bond angles at the P atoms vary in the sequence S=P–O > S=P–N > O–P–N > O–P–O as follows S1–P1–O2 115.07 (6)°, S1–P1–O1 114.90 (7)°, S1–P1–N1 112.87 (5)°, O2–P1–N1 107.30 (10)°, O1–P1–N1 106.34 (9)°, O1–P1–O2 99.12 (7)°. In one of the molecules of the structure (III), however, the maximum angle is one of the S=P–O angles [O2c–P1c–S1c 115.25 (5)°], but the S=P–N is only slightly larger than the other S=P–O angle, and the difference is within esd [O1c–P1c–S1c angle of 114.35 (5)° and N1c–P1c–S1c angle of 114.45 (5)°]. For this molecule, the minimum angle is 99.21 (6)° (O2c–P1c–O1c) and the two O–P–N angles follow the sequence noted. The sequence of bond angles at the P atom is also valid for the other three molecules in structure (III),

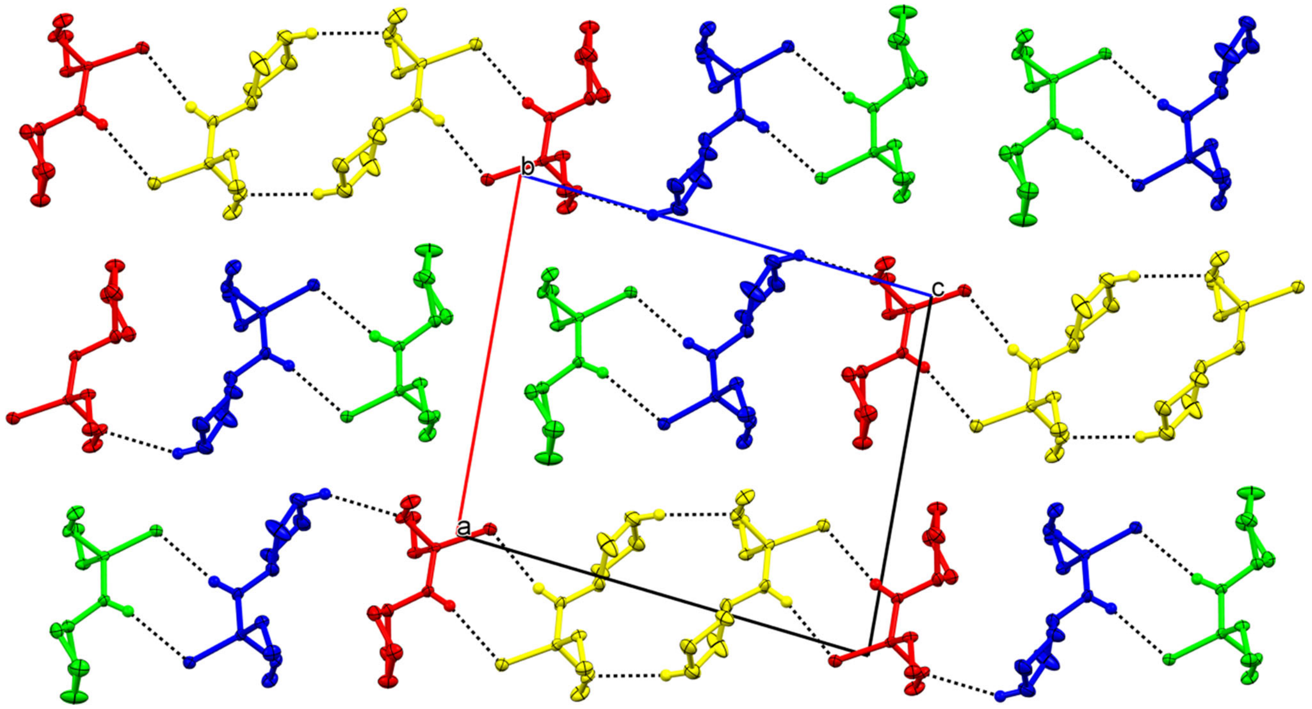

Fig. 9 A view of symmetrically independent non-centrosymmetric dimers in structure (III) is shown. Each dimer is built from two different N–H···S=P hydrogen bonds and the dimers are further connected via non-classical hydrogen bonds C–H···O. *Different colors* introduce symmetry independent molecules (Color figure online)

Table 8 Hydrogen bond geometry (Å, °) for compound (III)

D–H···*A*	*D*–H	H···*A*	*D*···*A*	*D*–H···*A*
N1a–H1n1a···S1b	0.880 (7)	2.720 (11)	3.5738 (14)	163.8 (15)
N1b–H1n1b···S1a	0.880 (8)	2.590 (11)	3.4449 (15)	164.3 (15)
N1c–H1n1c···S1d	0.880 (11)	2.665 (13)	3.5242 (15)	165.6 (14)
N1d–H1n1d···S1c	0.880 (11)	2.563 (14)	3.4169 (15)	164.0 (14)

with the maximum/minimum values of 115.37 (5)°/98.85 (6)° for P1a, 115.27 (5)°/99.33 (6)° for P1b and 115.43 (5)°/99.15 (6)° for P1d. In structures (II) and (III), the bond angle sums at the nitrogen atoms correspond to the planar geometry, for example, 359 (2)° in structure (II). Similar to compound (I), in compounds (II) and (III), the P–O–C angles are close to 120°: 119.05 (13)° and 119.53 (11)° in compound (II) and within 118.71 (10)° to 119.61 (10)° in four independent molecules in structure (III).

In structure (II), the N–H unit and P=S group adopt a *syn* orientation with respect to each other which is a suitable orientation for forming a centrosymmetric hydrogen-bonded dimer through intermolecular N–H···S=P hydrogen bonds (Fig. 8; Table 7). The orientations of N–H unit and P=S group in four symmetry independent molecules of the structure (III) are also *syn*. Hence, two symmetrically independent non-centrosymmetric dimers exist in the structure with each dimer built through two different N–H···S=P hydrogen bonds between two symmetry independent molecules (Fig. 9; Table 8).

Compound (IV) is the first diffraction study of a salt with an [S]P[O][O]–O–P[O][O][S] skeleton in the anion component, Fig. 10. It should be mentioned that through a search of (S)P(O)(O)(O) on the CSD, the structures of the following salts were found: BOKSUP [36], HAXRAZ [37] and MAXDOG [38]. Moreover, there are two zwitterionic structures GEYMUS [39] and KIVFAW [40] in the CSD.

The asymmetric unit of (IV) is composed of two symmetrically independent [2-Cl-$C_6H_4CH_2NH_3$]$^+$ cations and one [{[CH_3S]P[O][O]}$_2$O]$^{-2}$ dianion (Fig. 10). The main differences of the cations are reflected in the torsion angles N1a–C7a–C2a–C1a [80.0 (5)°] and N1b–C7b–C2b–C1b [−91.8 (6)°]. In the dianion, the P atoms are bonded in a distorted tetrahedral P(O)(O)(O)(S) environment in which the two (CH_3S)P(O)(O) parts are bridged via an O atom. The P1–O3 [1.618 (3) Å] and P2–O3 [1.614 (3) Å] bond

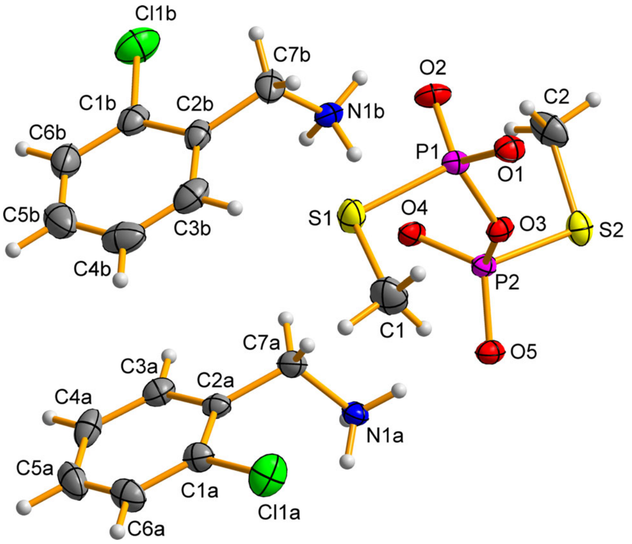

Fig. 10 Displacement ellipsoid plot (50 % probability) is shown for the asymmetric unit of (IV) with atom numbering scheme. H atoms are drawn as spheres of arbitrary radii

Table 9 Hydrogen bond geometry (Å, °) for compound (IV)

D–H···*A*	*D*–H	H···*A*	*D*···*A*	*D*–H···*A*
N1a–H1n1a···O5	0.88 (4)	2.00 (4)	2.844 (4)	160 (4)
N1a–H2n1a···O2^{a}	0.88 (3)	1.91 (4)	2.719 (5)	151 (5)
N1a–H3n1a···O1^{b}	0.88 (4)	1.90 (4)	2.779 (5)	173 (5)
N1b–H1n1b···O1^{c}	0.88 (3)	2.03 (3)	2.835 (4)	151 (4)
N1b–H2n1b···O5^{b}	0.88 (4)	1.91 (4)	2.780 (5)	170 (4)
N1b–H3n1b···O4	0.88 (4)	1.81 (4)	2.685 (5)	177 (5)

Symmetry codes: ^{a} $x - 1$, y, z; ^{b} $-x + 1$, $y - 1/2$, $-z + 2$; ^{c} $-x + 2$, $y - 1/2$, $-z + 2$

lengths and P1–O3–P2 angle [132.6 (2)°] are standard for the P–O–P fragment, such as reported in {[(CH$_3$)$_2$N][4–CH$_3$–C$_6$H$_4$–O]P(O)}$_2$(O) DUPCOH [41] and {[*tert*-C$_4$H$_9$NH]$_2$P(O)}$_2$O HAXQOO [42]. The C–S–P angles [99.0 (2)° and 100.9 (2)°] are in accordance with the angles of S atoms within a di-coordinated [P]S[*Y*] environment and are closer than the C–O–P angles (discussed in the section of CSD analysis).

In the crystal, the cations and dianions are hydrogen-bonded to each other, through N–H···O hydrogen bonds, in a two-dimensional network parallel to the *ab* plane (Fig. 11; Table 9), so that all of the six N–H units of two independent cations and four of the oxygen atoms of

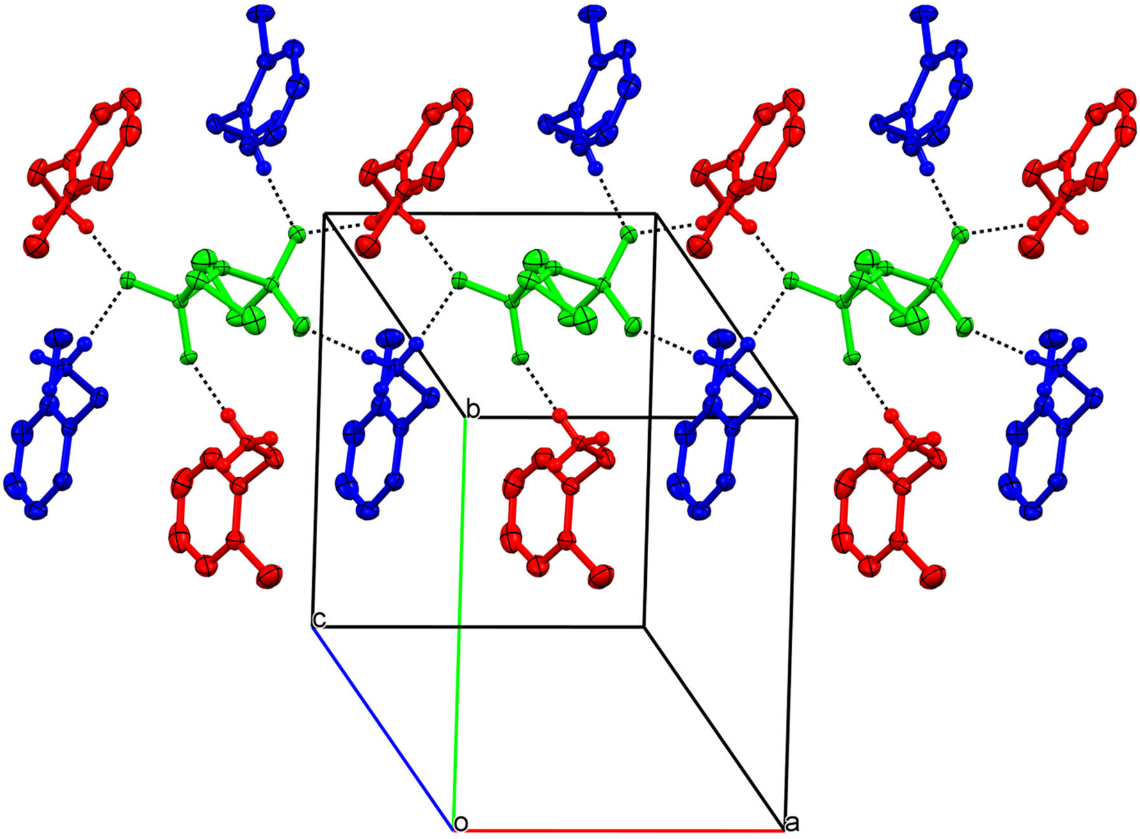

Fig. 11 Crystal packing of the structure (IV), the N–H···O=P hydrogen bonds are shown as *dashed lines*. Dianion is shown as *green color* and two symmetry independent cations are represented as *blue* and *red colors* (Color figure online)

dianion, apart from the bridging O atom, take part in hydrogen bond pattern. In this aggregation, each dianion is hydrogen-bonded to six neighboring cations, whereas each cation is hydrogen-bonded to three adjacent dianions. Due to cooperating of smaller numbers of hydrogen bond acceptors with respect to the number of hydrogen bond donors, two of the oxygen atoms of each dianion act as a double-hydrogen bond acceptor [12] to form $(N–H\cdots)_2O$ groups. The strong positive/negative charge-assisted hydrogen bonds (for a definition of different types of hydrogen bonds, see [43]) exist in the title salt, especially received by O2 and O4 atoms, which have relatively short distances of donor…acceptor. The $(N–H\cdots)_2O$ hydrogen bonds received by the O1 and O5 atoms are relatively weaker in this structure due to the anti-cooperativity effect [44] in the atoms which act as a double-hydrogen bond acceptors in the crystals.

Spectroscopic study (NMR, IR)

The chemical structures of compounds (I), (II), (III) and (IV) are given in Schemes 1, 2, 3 and 4, respectively. The $^{31}P\{^1H\}$ signals of compounds (I) and (II) (in DMSO-d_6) are revealed at −1.49 and 74.83 ppm, respectively. The ^{31}P and ^1H NMR experiments of compound (III) were previously reported (in $CDCl_3$), and the $^{31}P\{^1H\}$ signal in the present work at 75.16 ppm is in accordance with the published value (74.52 ppm) [19]. In the ^1H NMR spectrum of (I), two doublet signals at 7.60 ($J_{H–P} = 3.9$ Hz) and 7.92 ($J_{H–P} = 41.2$) ppm are related to the NH protons of the P(O)NHNH moiety. The considerable difference in coupling constants is similar to that was observed in compounds with a PNHNH fragment, like for example in $(CH_3CH_2O)_2P(S)(NHNHC_6H_5)$ with $J_{H–P} = 3.9$ and 43.0 Hz [6]. In the ^1H NMR experiments of (II) and (III), the hydrogen atoms of $–OCH_3$ groups show the coupling with the P atom ($^3J = 13.6$ Hz for both (II) and (III), the published value of 12.0 Hz for (III) [19]). The CH proton of $–CH(CH_3)_2$ group indicates a ddh fine structure due to the coupling with P atom, NH proton and the hydrogen atoms of two adjacent CH_3 groups. The NH protons of (II) and (III) are revealed at 5.45 and 5.55 ppm, respectively, both signals with a dd pattern, similar to the literature value of 3.72 for (III) in $CDCl_3$ with a dd pattern [19].

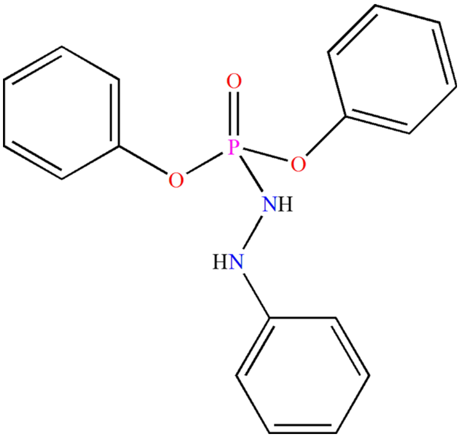

Scheme 1 Chemical structure of $P(O)(OC_6H_5)_2(NHNHC_6H_5)$

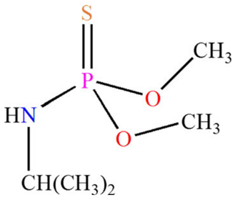

Scheme 2 Chemical structure of $P(S)(OCH_3)_2(NHCH(CH_3)_2)$

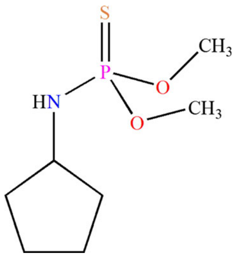

Scheme 3 Chemical structure of P(S)$(OCH_3)_2$(NH-*cyclo*-C_5H_9)

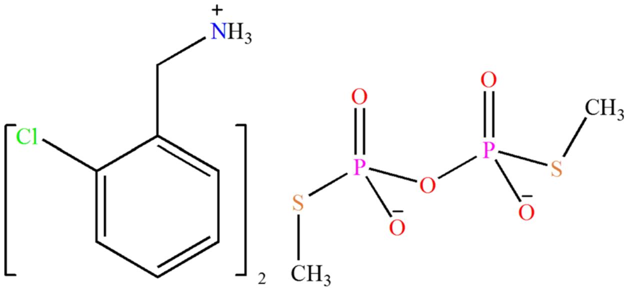

Scheme 4 Chemical structure of $[2\text{-Cl-}C_6H_4CH_2NH_3]_2[(CH_3S)P(O)(O)–O–P(O)(O)(SCH_3)]$

In the ^{13}C NMR spectrum of (I), the doublet signals at 150.57 ($^2J_{C–P} = 6.9$ Hz) and 120.35 ($^3J_{C–P} = 4.7$ Hz) ppm are, respectively, assigned to the *ipso*- and *ortho*-carbon atoms of the OC_6H_5 group and the other doublet signal at 149.59 ppm ($^3J_{C–P} = 4.8$ Hz) is assigned to the *ipso*-carbon atom of the $NHNHC_6H_5$ group. The chemical shifts and coupling constants values of (I) are in accordance with the values published [20] with a few differences due to the amount of solute in NMR solvent.

For (II) and (III), the doublet signals at 52.62 ($^2J = 5.1$ Hz) and 52.57 ($^2J = 4.9$ Hz) ppm are assigned to the carbon atoms of related OCH_3 groups, respectively [the assignment of the ^{13}C NMR was performed by running 2D HSQC experiment]. Furthermore, for compound (II), two doublet signals at 43.82 and 24.68 ppm are assigned to the CH and CH_3 carbon atoms of the $–CH(CH_3)_2$ group, respectively, with $|^3J_{C\text{–}P}| = 5.7$ Hz > $|^2J_{C\text{–}P}| = 1.7$ Hz. For compound (III), the doublet signals at 53.37 and 33.80 ppm are assigned to the carbon atoms with two and three bonds separations from the P atom, showing $|^3J_{C\text{–}P}| = 5.7$ Hz > $|^2J_{C\text{–}P}| = 2.3$ Hz.

The NH vibration stretching frequencies of compound (I) centered at 3296 and 3211 cm^{-1} are appeared at the lower wave numbers with respect to those of compounds II (3312 cm^{-1}) and (III) (3314 cm^{-1}), due to the stronger N–H···O=P hydrogen bond in (I) with respect to weaker N–H···S=P hydrogen bonds in (II) and (III). For (IV), a broad bond is observed within 2170–3147 cm^{-1} attributed to the NH stretching frequencies involved in hydrogen bonding.

Supplementary data

CCDC numbers of (I), (II), (III) and (IV) are 1,469,940, 1,469,941, 1,469,942 and 1,469,943, respectively. These data can be obtained free of charge via http://www.ccdc.cam.ac.uk/conts/retrieving.html, or from the Cambridge Crystallographic Data Centre, 12 Union Road, Cambridge CB2 1EZ, UK; fax: (+44) 1223-336-033, or e-mail: deposit@ccdc.cam.ac.uk.

Acknowledgments Financial support of this work by Zanjan Branch, Islamic Azad University is gratefully acknowledged. The X-ray part of the work was carried out with the support of X-ray Diffraction and Bio-SAXS Core Facility of CEITEC, and the ASTRA lab established within the Operation program Prague Competitiveness—project CZ.2.16/3.1.00/24510.

References

1. Quin LD (2000) A guide to organophosphorus chemistry. Wiley, Hoboken
2. Balali-Mood M, Abdollahi M (2014) Basic and clinical toxicology of organophosphorus compounds. Springer, London
3. Pourayoubi M, Toghraee M, Divjakovic V, van der Lee A, Mancilla Percino T, Leyva Ramírez MA, Saneei A (2013) Acta Crystallogr B 69:184–194
4. Pourayoubi M, Toghraee M, Zhu J, Dušek M, Bereciartua PJ, Eigner V (2014) CrystEngComm 16:10870–10887
5. Tarahhomi A, Pourayoubi M, Golen JA, Zargaran P, Elahi B, Rheingold AL, Leyva Ramírez MA, Mancilla Percino T (2013) Acta Crystallogr B 69:260–270
6. Pourayoubi M, Abrishami M, Eigner V, Nečas M, Dušek M, Delavar M (2014) Acta Crystallogr C 70:1147–1152
7. Raissi Shabari A, Pourayoubi M, Marandi P, Dušek M, Eigner V (2015) Acta Crystallogr C 71:338–343
8. Pourayoubi M, Saneei A, Dušek M, Rostami SA, Crochet A, Kučeraková M (2015) J Iran Chem Soc 12:2093–2103
9. Saneei A, Pourayoubi M, Crochet A, Fromm KM (2016) Acta Crystallogr C 72:230–233
10. Pourayoubi M, Toghraee M, Butcher RJ, Divjakovic V (2013) Struct Chem 24:1135–1144
11. Groom CR, Bruno IJ, Lightfoot MP, Ward SC (2016) Acta Crystallogr B 72:171–179
12. Pourayoubi M, Nečas M, Negari M (2012) Acta Crystallogr C 68:o51–o56
13. Pourayoubi M, Izadyar M, Elahi B, Parvez M (2013) J Mol Struct 1034:354–362
14. Pourayoubi M, Jasinski JP, Shoghpour Bayraq S, Eshghi H, Keeley AC, Bruno G, Amiri Rudbari H (2012) Acta Crystallogr C 68:o399–o404
15. Pourayoubi M, Rostami Chaijan M, Padelková Z, Ružicka A (2013) Phosphorus Sulfur 188:224–231
16. Gholivand K, Pourayoubi M, Shariatinia Z (2007) Polyhedron 26:837–844
17. Schranz I, Grocholl L, Carrow CJ, Stahl L, Staples RJ (2008) J Organomet Chem 693:1081–1095
18. Bock H, Baltin E (1965) Chem Ber Jahrg 98:2844–2854
19. Gupta AK, Dubey DK, Sharma M, Kaushik MP (2007) Org Prep Proced Int 39:297–305
20. Al-Rawi JMA, Behnam GQ, Ayed N (1983) Org Magn Reson 21:75–77
21. Franke HG (1975) US Patent, 3,917,755
22. Wan J, Zhan C-G (1995) Spectrochim Acta A 51:1665–1669
23. Palatinus L, Chapuis G (2007) J Appl Crystallogr 40:786–790
24. Petříček V, Dušek M, Palatinus L (2014) Z Kristallogr 229:345–352
25. Rohlíček J, Hušák M (2007) J Appl Crystallogr 40:600–601
26. Flack HD (1983) Acta Crystallogr A 39:876–881
27. Litvinov IA, Struchkov YT, Arbuzov BA, Liakisheva LS, Gurariy LI, Mukmenev ET (1981) Phosphorus Sulfur 12:5–9
28. Duthu B, El Abed K, Houalla D, Wolf R, Jaud J (1992) Can J Chem 70:809–816
29. Weemers JJM, Wiecko J, Pidko EA, Weber M, Lutz M, Müller C (2013) Chem Eur J 19:14458–14469
30. Labadi I, Sillanpää R, Lönnberg H (1992) J Chem Soc Dalton Trans 765–767
31. Karolak-Wojciechowska J, Mikolajczyk M, Kielbasinski P, Sut A (1984) Phosphorus Sulfur 21:221–225
32. Karolak-Wojciechowska J, Wieczorek MW, Struchkov YT, Antipin MY, Mikolajczyk M, Kielbasinski P, Sut A (1983) Phosphorus Sulfur 17:141–151
33. Kennard O, Coppola JC, Wampler DL, Kerr KA (1979) Acta Crystallogr B 35:3000–3003
34. Sá MM, Silveira GP, Bortoluzzi AJ, Padwa A (2003) Tetrahedron 59:5441–5447
35. Bernstein J, Davis RE, Shimoni L, Chang N-L (1995) Angew Chem Int Ed Engl 34:1555–1573
36. Betzel C, Loewus D, Saenger W (1983) Acta Crystallogr C 39:270–273
37. Fawcett J, Harger MJP, Russell DR, Sreedharan-Menon R (1993) J Chem Soc Chem Commun 1826–1828
38. Hummel M, Sixta H, Froschauer C, Weber HK, Kahlenberg V, Laus G, Schottenberger H (2010) CSD Commun, Private Commun in CSD (refcode MAXDOG)
39. Karle JM, Karle IL (1988) Acta Crystallogr C 44:1218–1221
40. Karle JM, Karle IL (1991) Acta Crystallogr C 47:1242–1245
41. Pourayoubi M, Ghadimi S, Ebrahimi Valmoozi AA (2010) Acta Crystallogr E 66:o450
42. Pourayoubi M, Tarahhomi A, Karimi Ahmadabad F, Fejfarová K, van der Lee A, Dušek M (2012) Acta Crystallogr C 68:o164–o169
43. Gilli P, Bertolasi V, Ferretti V, Gilli G (1994) J Am Chem Soc 116:909–915
44. Steiner T (2002) Angew Chem Int Ed 41:48–76